

# Synthesis of Cubic Hybrid Organic–Inorganic Mesoporous Structures with Dodecahedral Morphology from a Binary Surfactant Mixture

M. P. Kapoor and S. Inagaki\*

Toyota Central R&D Laboratories, Inc., Nagakute, Aichi 480-1192, Japan

Received April 8, 2002. Revised Manuscript Received June 3, 2002

Synthesis of a cubic ethane–silica hybrid organic–inorganic mesoporous material using a binary surfactant mixture is reported. The system consists of ethane-bridged organosilica (BTME), polyoxyethylene alkyl ether [ $C_{12}(EO)_4$ ; Brij 30], and the octadecyltrimethylammonium chloride ( $C_{18}TMACl$ ) surfactants in a basic medium. Powder X-ray diffraction analysis along with transmission electron microscope observation revealed a cubic symmetry of the mesophase and is consistent with the  $Pm\bar{3}n$  space group. Scanning electron microscope micrographs of material exhibit a well-defined crystal-like dodecahedral morphology with a uniform particle size of 5  $\mu\text{m}$ . Spectroscopic analyses confirmed that an ethane fragment is covalently linked to silica in surfactant-free material. The nitrogen adsorption isotherm shows a type-IV isotherm with a pore diameter of 28 Å and a Brunauer–Emmett–Teller surface area of 744  $\text{m}^2\text{g}^{-1}$ . The presented BTME–alkyltrimethylammonium– $C_{12}(EO)_4$ –NaOH– $H_2O$  system greatly facilitates the synthesis of cubic ( $Pm\bar{3}n$ ) hybrid mesoporous.

## Introduction

Recently, mesoporous material research has become a very active area and is highly regarded for its great potential for a range of applications in environmental and industrial processes. Several reports are available on the preparation by different routes and a fundamental understanding of the reaction processes using mesoporous material of novel chemical compositions. The size, charge, and shape of surfactant are important structure-determining parameters, especially, the local effective surfactant packing parameters<sup>1–3</sup> that can be defined as  $g = V/a_0l$ , where  $V$  is the total molecular volume of the hydrophobic surfactant chains plus any cosolvent species present,  $a_0$  is the effective surface headgroup area at the hydrophilic–hydrophobic micelle aggregate interface, and  $l$  is the kinetic surfactant tail length or the curvature elastic energy.

Usually, the effect of mixing unlike surfactants can be thought of as a simple average of two surfactant packing parameters. Huo et al.<sup>4</sup> used a mixture of different gemini surfactants  $C_{16-12-16}$  and  $C_{16-3-1}$  for a silicate mesophase synthesis where the products vary from MCM-48 (cubic,  $Ia\bar{3}d$ ) to SBA-2 (three-dimensional hexagonal  $P6_3/mmc$ ) through MCM-41 (two-dimensional hexagonal  $P6mm$ ) as the fraction of  $C_{16-3-1}$  increases in the mixture. Ryoo et al.<sup>5</sup> have obtained the cubic

( $Ia\bar{3}d$ ) mesoporous silica molecular sieve MCM-48 as an energetically favorable mesophase via a synthesis route using the surfactant mixtures of alkyltrimethylammonium bromides and polyoxyethylene alkyl ethers with sodium silicate as the silica source. As the synthesis parameters were varied, they monitored that mesoporous structures continuously changes from hexagonal to lamellar include the cubic ( $Ia\bar{3}d$ ) that appeared in the middle of the transition.

Recently, using the general class of compounds referred to as the organosilane compound  $(RO)_3Si-R^1-Si(OR)_3$ , a new class of poly(bridged silsesquioxane) mesoporous with integral organic functionality have been reported.<sup>6–9</sup> The organic constituent ( $R^1$ ) includes methylene, ethane, ethylene, benzene, and thiophene. This class of material necessarily incorporates the organic fragment into the framework as molecularly dispersed bridging ligands that enlarge the synergistic properties derived from the molecular-scale mixing of the organic and inorganic components. In this system, highly ordered mesoporous of two-dimensional hexagonal ( $P6mm$ ), cubic ( $Pm\bar{3}n$ ), and three-dimensional hexagonal ( $P6_3/mmc$ ) have been synthesized from ethane-bridged organosilica [ $(CH_3O)Si-CH_2-CH_2-Si(OCH_3)_3$ ; BTME] in the presence of alkyltrimethylammonium (ATMA) surfactant. The formation of cubic ( $Pm\bar{3}n$ ) and three-dimensional hexagonal ( $P6_3/mmc$ ) mesoporous is very unusual in an ATMA surfactant system because of the relatively smaller headgroup area of ATMA.

\* Corresponding author. E-mail: inagaki@mosk.tytlabs.co.jp. Fax: 81-561-63-8493. Tel: 81-561-63-6498.

(1) Zhao, D.; Huo, Q.; Feng, J.; Chmelka, B. F.; Stucky, G. D. *J. Am. Chem. Soc.* **1998**, *120*, 6024.

(2) Melosh, N. A.; Lipic, P.; Bates, F. S.; Wudl, F.; Stucky, G. D.; Fredrickson, G. H.; Chmelka, B. F. *Macromolecules* **1999**, *32*, 4332.

(3) Tanev, P. T.; Pinnavaia, T. J. *Science* **1996**, *271*, 1267.

(4) Huo, Q.; Margolese, D. I.; Stucky, G. D. *Chem. Mater.* **1996**, *8*, 1147.

(5) Ryoo, R.; Joo, S. H.; Kim, J. M. *J. Phys. Chem.* **1999**, *103*, 7435.

(6) Inagaki, S.; Guan, S.; Fukushima, Y.; Ohsuna, T.; Terasaki, O. *J. Am. Chem. Soc.* **1999**, *121*, 9611.

(7) Melde, B. J.; Holland, B. T.; Blanford, C. F.; Stein, A. *Chem. Mater.* **1999**, *11*, 3302.

(8) Asefa, T.; MacLachlan, M. J.; Coombs, N.; Ozin, G. A. *Nature* **1999**, *402*, 867.

(9) Yoshina-Ishii, C.; Asefa, T.; Coombs, N.; MacLachlan, M. J.; Ozin, G. A. *Chem. Commun.* **1999**, *402*, 867.

Therefore, these results suggest that different parameters determining the mesophase exist in the system using organosilica as a framework source. We have not yet had a report on applying a binary surfactant mixture to the hybrid organic–inorganic hybrid system.

Three-dimensional mesoporous materials synthesized from different templating routes<sup>10–13</sup> are of particular interest for applications such as chemical sensing or separation, catalysis, filtration, and encapsulation. There are very few examples in which mesoporous material shows a crystal-like well-defined morphology.<sup>14–16</sup> In this paper we describe the synthesis of cubic hybrid ethane–silica mesoporous structures with well-defined dodecahedral morphology using a binary surfactant mixture. The material designated as a hybrid mesoporous cubic (HMC) is indexed to the  $Pm\bar{3}n$  space group. The system consists of an ethane-bridged organosilica (BTME), octadecyltrimethylammonium chloride ( $C_{18}$ -TMACl), and the polyoxyethylene alkyl ether [ $C_{12}$ (EO)<sub>4</sub>; Brij-30] surfactants dissolved in a basic solution.

### Experimental Section

**Materials.** BTME [1,2-bis(trimethoxysilyl)ethane] was obtained from Shin-Etsu, and  $C_{18}$ TMACl and polyoxyethylene alkyl ether [ $C_{12}$ (EO)<sub>4</sub>; Brij-30] surfactants were obtained from Tokyo Kasei and Aldrich. All other solvents and reagents were purchased from Wako Chemicals.

**Instrumentation.** Formation of a mesostructure was confirmed with powder X-ray diffraction patterns (PXRD) obtained by using a Rigaku RINT-2200 diffractometer with Cu K $\alpha$  radiation (40 kV and 30 mA) from 1 to 10° 2 $\theta$ , 0.01 step and 1° 2 $\theta$ /min scan speed. Porosimetry measurements were determined using a quantachrome Autosorb-1 at 77 K. The samples were completely evacuated for 2 h at 50 °C before measurement. The pore size distributions were calculated using the Barrett–Joyner–Halenda (BJH) model from the adsorption branch isotherms.

Scanning electron microscope (SEM) images were obtained on a JEOL JSM-890 field emission scanning microscope with an acceleration voltage of 5 kV. The samples were coated with Au prior to measurement. A transmission electron micrograph (TEM) was obtained on a JEM-200CX with an acceleration voltage of 200 kV for both hexagonal and cubic symmetry planes.

The <sup>29</sup>Si and <sup>13</sup>C cross-polarization (CP) magic angle spinning (MAS) NMR spectra were obtained on a Bruker MSL-300WB spectrometer at 59.62 and 75.47 MHz for <sup>29</sup>Si and <sup>13</sup>C NMR, respectively. Chemical shifts for both <sup>29</sup>Si and <sup>13</sup>C NMR were referenced to trimethylsilane (TMS) at 0 ppm. Fourier transform infrared (FTIR) spectra of surfactant-free samples were recorded with a Nicolet Thermo-360 FT-IR. Thermogravimetric analysis (TGA) was carried out on a Rigaku Thermo Plus TG-8120 instrument with a program rate of 10 °C min<sup>-1</sup> in air as well as in nitrogen with a flow rate of 500 mL min<sup>-1</sup>.

**Synthesis of HMC-1.** In a typical synthesis procedure of hybrid cubic mesoporous material HMC-1, the mixture with

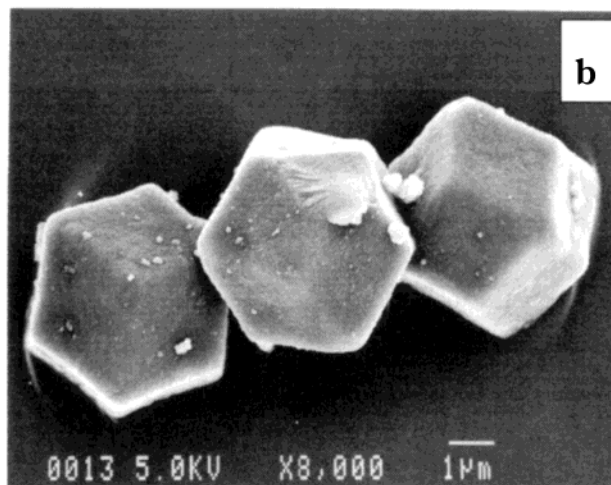
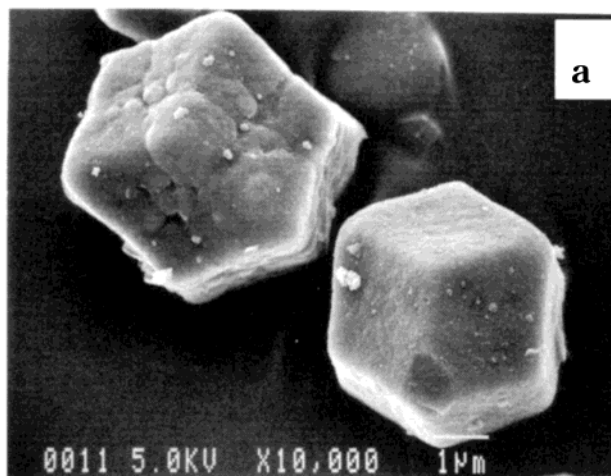


**Figure 1.** SEM images of ethane–silica hybrid mesoporous material (HMC-1) with cubic symmetry synthesized from mixed surfactants.

the following molar ratio was used: BTME, 1.0; surfactant [ $C_{12}$ (EO)<sub>4</sub>: $C_{18}$ TMACl = 0.15:0.85], 1.0; NaOH, 2.4; H<sub>2</sub>O, 350. First, both surfactants Brij-30 (1.5 mmol) and  $C_{18}$ TMACl (8.5 mmol) were mixed in 62 g of H<sub>2</sub>O under vigorous stirring and dissolved by heating at 40–50 °C. After complete dissolution of the surfactant, 5 g of a 6 N NaOH solution was added to the mixture and further stirred for at least 15 min. BTME (10 mmol) was then added, and stirring was continued for 18 h at room temperature while a precipitate formed. The solution was then autoclaved for hydrothermal synthesis at 90–95 °C for 24 h to increase the degree of condensation. Separation of a mesoporous solid was carried out by filtration, and the solid was washed thoroughly with a copious amount of distilled water and dried under evacuation at room temperature. The samples with the varied fraction of surfactant [ $C_{12}$ (EO)<sub>4</sub>: $C_{18}$ -TMACl = 0.10:0.90 (HMC-2) and 0.20:0.80 (HMC-3)] were also synthesized.

**Surfactant Extraction.** The surfactant was removed by a solvent extraction method. In a typical procedure, 1.0 g of an as-synthesized mesoporous material was stirred for 8 h at 50 °C in a HCl/ethanol solution (200 mL of ethanol contained 3 g of concentrated ~36 wt % HCl). The extraction process was then repeated. A weight loss of about 30–35% was obtained after a complete solvent extraction.

### Results and Discussion

**SEM Analysis.** SEM images of HMC-1 from different projections are shown in Figure 1. Particles are uniform

(10) Huo, Q.; Margolese, D. I.; Ciesla, U.; Feng, P.; Gier, T. E.; Sieger, P.; Leon, R.; Petroff, P. M.; Schuth, F.; Stucky, G. D. *Nature* **1994**, *368*, 317.

(11) Huo, Q.; Margolese, D. I.; Ciesla, U.; Demuth, D. G.; Feng, P.; Gier, T. E.; Sieger, P.; Forouzi, A.; Chmelka, B. F.; Schuth, F.; Stucky, G. D. *Chem. Mater.* **1994**, *6*, 1176.

(12) Zhao, D.; Feng, J.; Huo, Q.; Melosh, N.; Fredrickson, G. H.; Chmelka, B. F.; Stucky, G. D. *Science* **1998**, *279*, 548.

(13) Sakamoto, Y.; Kaneda, M.; Terasaki, O.; Zhao, D.; Kim, J. M.; Stucky, G. D.; Shin, H. J.; Ryoo, R. *Nature* **2000**, *408*, 449.

(14) Kim, J. M.; Kim, S. K.; Ryoo, R. *Chem. Commun.* **1998**, 259.

(15) Sayari, A. *J. Am. Chem. Soc.* **2000**, *122*, 6504.

(16) Guan, S.; Inagaki, S.; Ohsuna, T.; Terasaki, O. *J. Am. Chem. Soc.* **2000**, *122*, 5660.

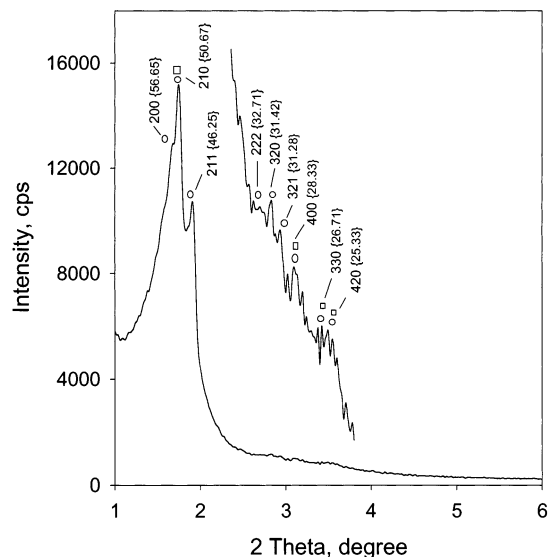


**Figure 2.** PXRD patterns of surfactant-free ethane–silica hybrid mesoporous material with cubic symmetry (HMC-1).

**Table 1. Indexing and *d*-Spacing Assignments for HMC-1**

<i>d</i> spacing (Å)		indexing	
observed	calculated	(○) $Pm\bar{3}n$	(□) $Ia\bar{3}d$
55.54	56.65	200	
50.67	50.67	210	210
45.92	46.25	211	221
	40.06		220
	35.83	310	
32.71	32.71	222	
31.10	31.42	320	
30.04	30.28	321	321
29.34	28.33	400	400
27.60	26.71	330	
25.83	25.33	420	420

in both size ( $\sim 5 \mu\text{m}$  in diameter) and shape consistent with a well-defined rhombic dodecahedral morphology with faces indexed as 110 planes. This morphology is somewhat different from those reported for a similar cubic ethane–silica mesophase that showed decaoctahedral shape with 6 squares and 12 hexagons indexed to  $\{100\}$  and  $\{110\}$  planes, respectively. This also suggests that particles are single crystals.

**PXRD Patterns and TEM Analysis.** Figure 2 shows a typical PXRD pattern for a cubic HMC-1 sample. Most of the peaks are well-fitted [especially the first three main peaks of (200), (210), and (211)] to the diffraction lines for a  $Pm\bar{3}n$ -type cubic structure with a unit cell  $a = 113 \text{ \AA}$ . Other peaks are also assignable to a cubic symmetry. The observed and calculated *d*-spacing values of all distinct peaks are listed in Table 1. For surfactant-free HMC-1, the *d* spacing of the most intense peak of (210) was  $50.7 \text{ \AA}$  and no considerable shrinkage was noticed after surfactant removal. Owing to the strong similarity between this diffractogram and that of SBA-1 ( $Pm\bar{3}n$ )<sup>10</sup> and cubic hybrid silica ( $Pm\bar{3}n$ ),<sup>16</sup> it is inferred that the structure of the present material was also identified as belonging to the same space group. This assignment was further confirmed by TEM especially because hybrid mesoporous materials are known to be capable of forming a variety of ordered and disordered structures with observable PXRD reflections and well-defined porosity. TEM images for different mesopore arrangements are shown in Figure 3. A

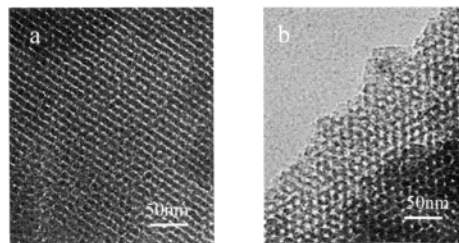


**Figure 3.** TEM micrograph of the extracted HMC-1 in different planes.

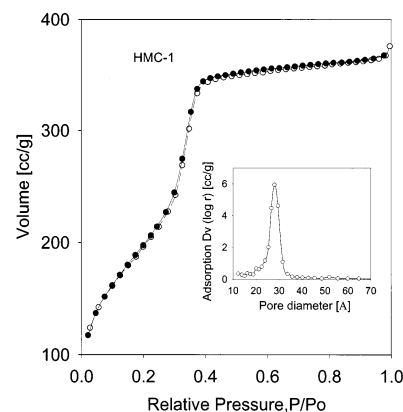


**Figure 4.**  $\text{N}_2$  adsorption–desorption isotherms for the extracted HMC-1 and BJH pore size distribution (inset). Open circle: adsorption. Closed circle: desorption.

regular arrangement of bright spots reveals that the mesoporous material is of the three-dimensional-cage type. Further, the TEM results also support the conclusion from XRD analysis that material has three-dimensional-cage-type symmetry.

**Porosity Measurements.** The corresponding  $\text{N}_2$  adsorption–desorption isotherm and pore size distribution are presented in Figure 4. The nitrogen adsorption isotherm of type IV, with a sharp increase in the adsorption at  $P/P_0 = 0.30\text{--}0.38$ , clearly indicates that the material has a uniform mesopore structure. The BJH pore diameter, Brunauer–Emmett–Teller (BET) surface area, and pore volume were  $28 \text{ \AA}$ ,  $744 \text{ m}^2 \text{ g}^{-1}$ , and  $0.62 \text{ cm}^3 \text{ g}^{-1}$ , respectively. From the observation of the nitrogen adsorption isotherm, we noticed that the pore size estimated by the BJH method is well under its estimation,<sup>17</sup> while the pore size distribution estimated using the NLDFT equilibrium model ( $\text{N}_2$  adsorption at  $77 \text{ K}$  on silica MCM type) was  $41 \text{ \AA}$ , quite close to the value calculated as defined in the literature.<sup>17</sup> The results clearly indicate that the HMC-1 material has a well-defined porous structure and uniform pore dimensions, as was also confirmed by TEM analysis.

**$^{29}\text{Si}$  MAS NMR and  $^{13}\text{C}$  CP-MAS NMR Studies.** The  $^{29}\text{Si}$  MAS NMR spectra of solvent-extracted HMC-1 exhibited two peaks at  $-66.3$  and  $-57.4$  ppm (Figure 5). The first peak ( $-66.3$  ppm) was assigned to  $\text{T}^3$  [ $\text{SiC}(\text{OSi})_3$ ], a fully condensed silicon, and the other to  $\text{T}^2$  [ $\text{SiC}(\text{OH})\text{--}(\text{OSi})_2$ ], a partially hydrolyzed silica species. No signals due to  $\text{SiO}_4$  species ( $Q^n$ ,  $n = 1\text{--}4$ ), indicate that all Si atoms are covalently connected to carbon atoms in the framework because complete cross-linking occurred in this material. No difference in the  $\text{T}^3/\text{T}^2$

(17) Kruk, M. Jaroniec, M. *Chem. Mater.* **2001**, *13*, 3169.



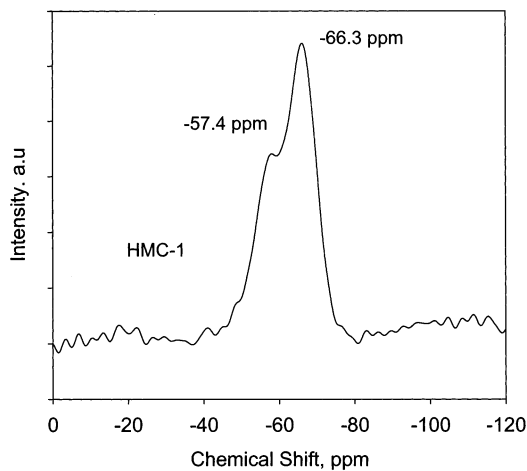


**Figure 5.**  $^{29}\text{Si}$  MAS NMR spectrum of surfactant-free HMC-1 mesoporous material.

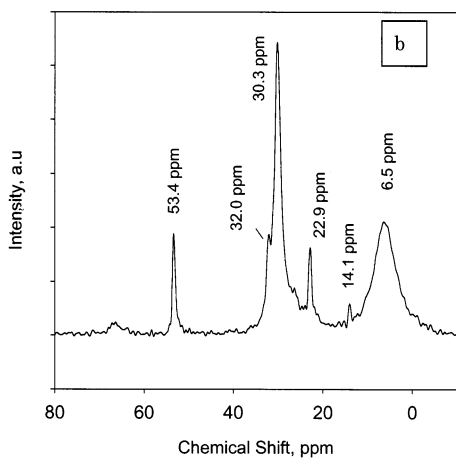
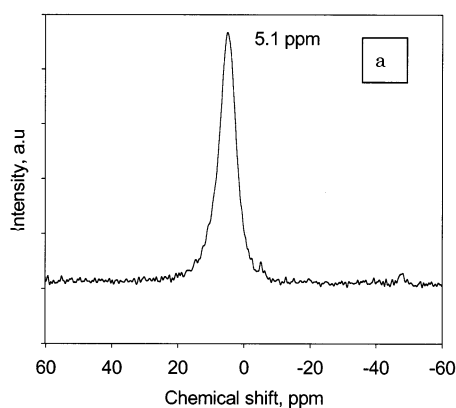


**Figure 6.**  $^{13}\text{C}$  CP-MAS NMR spectra of the (a) surfactant-free and (b) as-synthesized HMC-1 mesoporous material.

signal intensity ratio was noticed after surfactant removal, indicating absolutely no further condensation of organosilicates during the extraction with a HCl-ethanol solution. Evidently, the HMC-1 sample exhibited a high degree of framework cross-linking.

The  $^{13}\text{C}$  cross-polarization (CP) MAS NMR spectrum shows that after extraction (Figure 6a) the material exhibits a strong signal at 5.1 ppm, revealing that the ethane fragment is covalently linked to silica, composed of  $\text{SiO}_{1.5}\text{-CH}_2\text{-CH}_2\text{-Si O}_{1.5}$  units. No carbon signals due to  $\text{C}_{18}\text{TMACl}$  and  $\text{C}_{12}(\text{EO})_4$  surfactant were observed in the extracted sample as seen in the as-

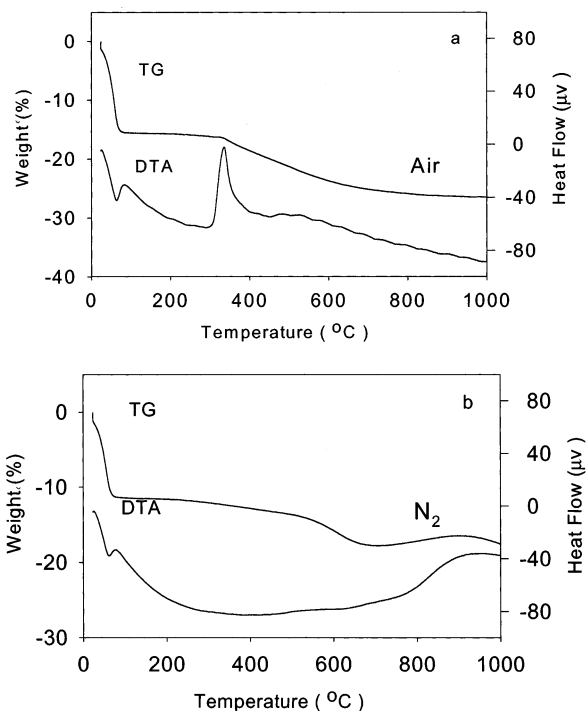


**Figure 7.** TGA and DTA measurements of hybrid mesoporous silica HMC-1 (a) in air and (b) in a nitrogen atmosphere.

synthesized sample (Figure 6b), suggesting complete removal of the surfactant from the mesoporous material. Similarly, the FTIR spectra of HMC-1 revealed (not shown) that, after removal of surfactant by the extraction process, the organic group ( $\text{-CH}_2\text{-CH}_2\text{-}$ ) remained intact as indicated by the vibrations at 1423, 1267, and  $1157\text{ cm}^{-1}$  along with the vibration at the fingerprint region between  $600$  and  $800\text{ cm}^{-1}$ .

**Thermal Properties Measurement.** The quantitative determination of the functional group contents of the hybrid mesoporous silica after extraction of the surfactant species was performed with TGA and differential thermal analysis (DTA) in air as well as in a nitrogen atmosphere. The TGA and DTA analyses of the HMC-1 sample in air show a first weight loss below  $100^\circ\text{C}$  due to desorption of physisorbed water (about 15 wt %; see Figure 7a). This is followed by a gradual decrease in the weight at temperatures between  $300$  and  $800^\circ\text{C}$ , which corresponds to the loss of ethane fragments in the pore wall. The DTA curve in Figure 8a is accompanied by a sharp peak centered at  $338^\circ\text{C}$ , indicating that most of the ethane was decomposed at the initial stage. The total loss for the ethane fragment alone was about 10 wt %. On the other hand, the TGA/DTA spectra of HMC-1 in a nitrogen atmosphere (Figure 7b) showed a comparatively lower initial weight decrease (initial water loss of  $\sim 11$  wt %) The decomposition of ethane fragments began over  $400^\circ\text{C}$ , and the total loss of the ethane fragment was  $\sim 6$  wt %. In addition, a surprising increase in weight was observed at relatively higher temperatures (between  $800$  and  $950^\circ\text{C}$ ), most likely because of the reaction of a partially decomposed bridging organic group with nitrogen. It is also noteworthy that the sample weight at a temperature above  $800^\circ\text{C}$  is comparatively larger under nitrogen than air. This also suggests that an appreciable amount of carbonaceous deposit forms under a nitrogen atmosphere and is not thermodesorbed even at  $1000^\circ\text{C}$ .

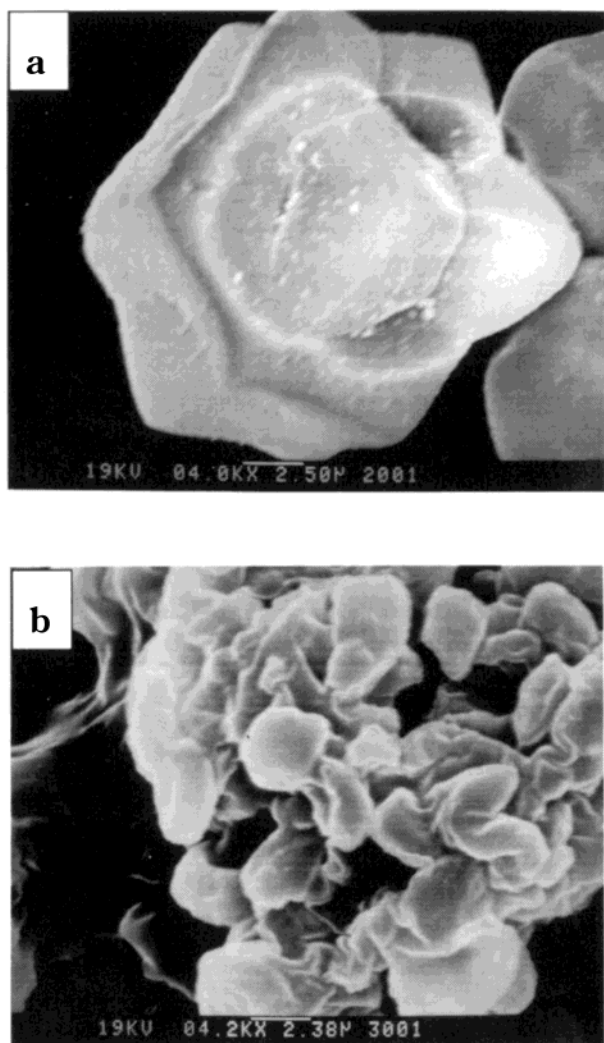


**Figure 8.** SEM images of ethane–silica hybrid mesoporous material synthesized from the different molar ratios of mixed  $C_{12}(EO)_4$  and  $C_{18}TMACl$  surfactants: (a) 0.10:0.90 (HMC-2); (b) 0.20:0.80 (HMC-3).

On the other hand, the observed weight gain could also be attributed to the silicon nitride or silicon oxynitride formation. The details of such a nitride formation have not been analyzed yet.

**Influence of Synthesis Parameters on Mesophases.** In addition, samples were also prepared with different  $C_{18}TMACl$  and  $C_{12}(EO)_4$  ratios using the same procedure, demonstrated for sample HMC-1. In the synthesis, the different amounts of  $C_{18}TMACl$  surfactant were replaced by those of  $C_{12}(EO)_4$  surfactant. The product order and morphology strongly depended on the hydrolysis and condensation kinetics of the silica precursor (BTME) in the presence of different ratios of mixed surfactants. When  $C_{12}(EO)_4/C_{18}TMACl$  surfactant ratios of 0.10/0.90 were used, the cubic symmetry could not be obtained (HMC-2). The XRD spectra were quite broad and noncompatible with either hexagonal or cubic symmetry. The SEM image of the sample exhibits the deformed growth of the cubic section (flowerlike), clearly indicating that the material has the deformed mixed morphology somewhat intermediate to hexagonal and cubic symmetry (Figure 8a). While the sample was synthesized from a 0.20/0.80 molar ratio of  $C_{12}(EO)_4/C_{18}TMACl$  surfactants, the morphologies were quite

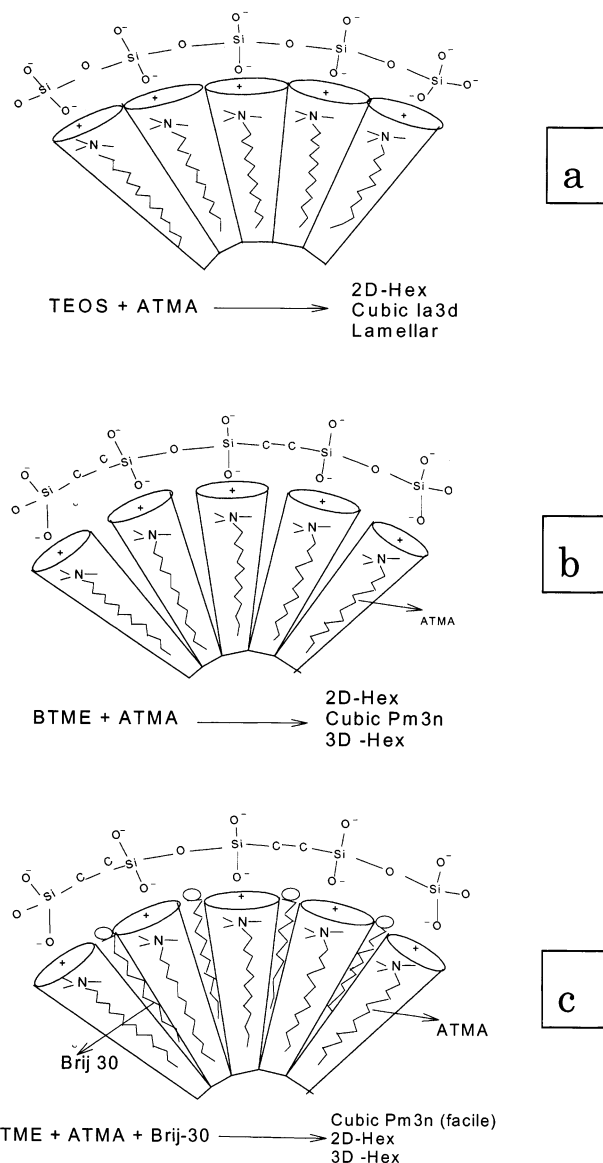


**Figure 9.** Proposed mechanism of mesophase formation with a binary surfactant mixture.

different from those observed previously (HMC-3). The structural order of this material was very poor, and wormlike morphology was observed (Figure 8b). Compared to the HMC-1 sample, the BET surface areas were also somewhat lowered with broad pore size distributions.

**Plausible Mechanism and Hypothesis for Mesophase Formation with Binary Surfactant Mixtures.** ATMA surfactant alone usually forms two-dimensional hexagonal ( $P6mm$ ), cubic ( $Ia3d$ ), and lamellar mesophases in a surfactant–water binary system<sup>18</sup> and also in an inorganic–surfactant–water ternary system.<sup>19</sup> The typical geometry of BTME and the formation of unusual mesophases in the BTME–ATMA– $C_{12}(EO)_4$ –NaOH– $H_2O$  system are shown in Figure 9. In the silica-based mesophase synthesis system, the phase behavior of the binary surfactant

(18) Vartuli, J. C.; Schmitt, K. D.; Kresge, C. T.; Roth, W. J.; Leonowicz, M. E.; McCullen, S. B.; Hellring, S. D.; Beck, J. S.; Schlenker, J. L.; Olson, D. H.; Sheppard, E. W. *Chem. Mater.* **1994**, *6*, 2317.

(19) Tiddy, G. J. T. *Phys. Rep.* **1980**, *57*, 1.

mixture system turns more complicated as a result of the formation of surfactant–silica mesoporous structures in the aqueous solution. Also, the choice of an appropriate silica source is very important to control the effective headgroup area as well as surface curvature that help to obtain the desired mesophases.

In the conventional TEOS–ATMA–H<sub>2</sub>O mesophase system (Figure 9a; TEOS as a silica source), the anion charge density is usually very high compared to the effective headgroup area and silicate anions in the solution are strongly attracted by electrostatic attraction surrounding the headgroups of cationic surfactant (C<sub>18</sub>TMACl) micelles. The motions of surfactant molecules are limited to a certain degree, and polymerization of silicate strongly influences the packing of the inorganic–organic array. Addition of nonionic surfactant C<sub>12</sub>(EO)<sub>4</sub> decreases the surface curvature around the surfactant micelles, and the effective headgroup area becomes comparatively small (very tight head-to-tail micelle packing) that resulted in a phase transition from hexagonal to cubic (*Ia3d*).<sup>5</sup>

In the BTME–ATMA–NaOH–H<sub>2</sub>O system (see Figure 9b), the typical geometry of an ethane-bridged organosilica (BTME) molecule resulted in the formation of unusual mesophases. The use of BTME remarkably decreases the anion charge density on the polymerized species and the headgroup area becomes effectively large and that favors the formation of two-dimensional hexagonal mesophases (*P6mm*), and also under very crucial synthesis parameters, the cubic (*Pm3̄n*) mesophases can be obtained (BTME–C<sub>16</sub>TMA–NaOH–H<sub>2</sub>O system).<sup>16</sup>

Addition of the C<sub>12</sub>(EO)<sub>4</sub> surfactant into the BTME–C<sub>18</sub>TMACl system does not much affect the surface curvature around the micelle because of the relatively loose head-to-tail micelle packing. In this case neutral surfactant has no strong interaction with the silicate anions, and its presence (as a space filler) in the micelles simply leads to a dilution of the silicate anions at the

surface. It is also possible that the C<sub>12</sub>(EO)<sub>4</sub> surfactant penetrates into the hydrophobic and palisade regions of the surfactant arrays and thereby induces a structural rearrangement of the surfactant phase to re-optimize the interface charge density matching and surfactant packing.

Therefore, under the described synthesis conditions, the cubic (*Pm3̄n*) mesophases (Figure 9c; BTME–ATMA–C<sub>12</sub>(EO)<sub>4</sub>–NaOH–H<sub>2</sub>O system) can be formed very easily because the low surface concentration and subsequent polymerization may well lead to a contraction of the micellar surface, resulting in phase transition from two-dimensional hexagonal (*P6mm*) to cubic (*Pm3̄n*), indicating that the geometry of the framework source and surfactant packing parameters are very important to the determination of the mesophase. Therefore, the overall morphology of the mesophases is qualitatively described by the dimensionless effective surfactant packing parameters. This also explains why, in the case of the BTME–ATMA–NaOH–H<sub>2</sub>O system,<sup>16</sup> the decaoctahedral morphology was observed, while in the present BTME–ATMA–C<sub>12</sub>(EO)<sub>4</sub>–NaOH–H<sub>2</sub>O system, the dodecahedral morphology is evidently observed.

### Conclusions

In summary, very high quality cubic hybrid mesoporous silica (*Pm3̄n*) with well-defined crystals of truncated rhombic dodecahedra can be prepared using bridged organosilica species as precursors and a binary mixture of C<sub>18</sub>TMACl and C<sub>12</sub>(EO)<sub>4</sub> (Brij-30) surfactant. The present BTME–ATMA–C<sub>12</sub>(EO)<sub>4</sub>–NaOH–H<sub>2</sub>O system greatly facilitates the synthesis of cubic (*Pm3̄n*) hybrid mesophases and enlarges the synthesis parameter window. Material can be synthesized by simply using hydrothermal conditions. Further, considering the use of different surfactant mixtures, the findings of mesophases with new structures are anticipated.

CM020345B